ELSEVIER

Biophysical Chemistry 122 (2006) 5 – 15

Biophysical Chemistry

http://www.elsevier.com/locate/biophyschem

Ability of spermine to differentiate between DNA sequences—Preferential stabilization of A-tracts

Mayank M. Patel *, Thomas J. Anchordoquy

Department of Pharmaceutical Sciences, School of Pharmacy—C238, University of Colorado Health Sciences Center, 4200 E. Ninth Avenue, Denver, CO 80262, United States

Received 17 January 2006; received in revised form 7 February 2006; accepted 7 February 2006
Available online 28 February 2006

Abstract

The regulatory roles fulfilled by polyamines by governance of chromatin structure are made possible by their strong association with cellular DNA, and hence by their ability to modulate DNA structure and function. Towards this end, it is crucial to understand the manifestation of sequence-dependent polyamine binding at the secondary and tertiary structural levels of DNA. This study utilizes circular dichroism (CD) and isothermal titration calorimetry (ITC) to address this relationship by using 20 bp oligonucleotides with sequences–poly(dA):poly(dT), poly (dAdT):poly(dAdT), poly(dG):poly(dC), poly(dGdC):poly(dGdC)–that yield physiologically relevant structures, and poly(dIdC):poly(dIdC). CD studies show that at physiological ionic strength (150 mM NaCl), spermine preferentially stabilizes A-tracts, and increases flexibility of the G-tract oligomer; the latter is also suggested by the larger change in entropy (ΔS) of spermine binding to G-tracts. Given the chromatin destabilizing property of these sequences, these findings suggest a role for spermine in stabilization of non-nucleosomal A-tracts, and a compensating mechanism for incorporation of G-tracts in the chromatin structure. Other implications of these findings in sequence dependent DNA packaging are discussed.
© 2006 Elsevier B.V. All rights reserved.

Keywords: Sequence-specific spermine–DNA binding; Isothermal Titration Calorimetry (ITC); A-tracts; G-tracts; Thermodynamics of spermine–DNA binding

1. Introduction

The omnipresence of polyamines in mammalian cells has implications in functions ranging from gene expression to cell growth regulation [1–4]. These functions are made possible by intracellular concentrations of polyamines, such as spermine and spermidine, in the millimolar range—owing to their charged state at physiological pH they are substantially bound to nucleic acids, thereby modulating the biological activity of DNA [5,6]. Spermine, a tetracationic polyamine, binding to DNA manifests itself at the secondary and tertiary structural levels, thereby influencing transcriptional functionalities by affecting the ability of other ligands, e.g., transcription and regulatory enzymes, to compete for binding sites on DNA strands. This can be affected by induction of a B → Z transition in polynucleotides by spermine [7–9]. The presence and concentration of spermine in the chromatin can stabilize [10], or destabilize double stranded DNA, and thereby influence chromosomal DNA packaging [4,11–13]. Using this polyamine as a model, we strive to understand the relationship between DNA secondary structure, as influenced by nucleotide sequence, and thermodynamics of spermine binding to duplex DNA. A deeper understanding of such interactions would also aid in establishing the role of nucleotide sequence in multivalent cation-induced DNA packaging for gene delivery applications.

It is imperative to study spermine–DNA interactions as a function of nucleotide sequence because of its role in chromatin structure and in other biological functions: oligopurines tracts of 10 or more contiguous residues are found 4 times more frequently in the β-globin region of human genomic DNA than would be expected with a random distribution of sequences [14]; 10 to 30 bp long A-tracts occur frequently in eukaryotic

* Corresponding author. Tel.: +1 303 315 0359; fax: +1 303 315 6281.
E-mail address: mayank.patel@uchsc.edu (M.M. Patel).

0301-4622/$ - see front matter © 2006 Elsevier B.V. All rights reserved.
doi:10.1016/j.bpc.2006.02.001

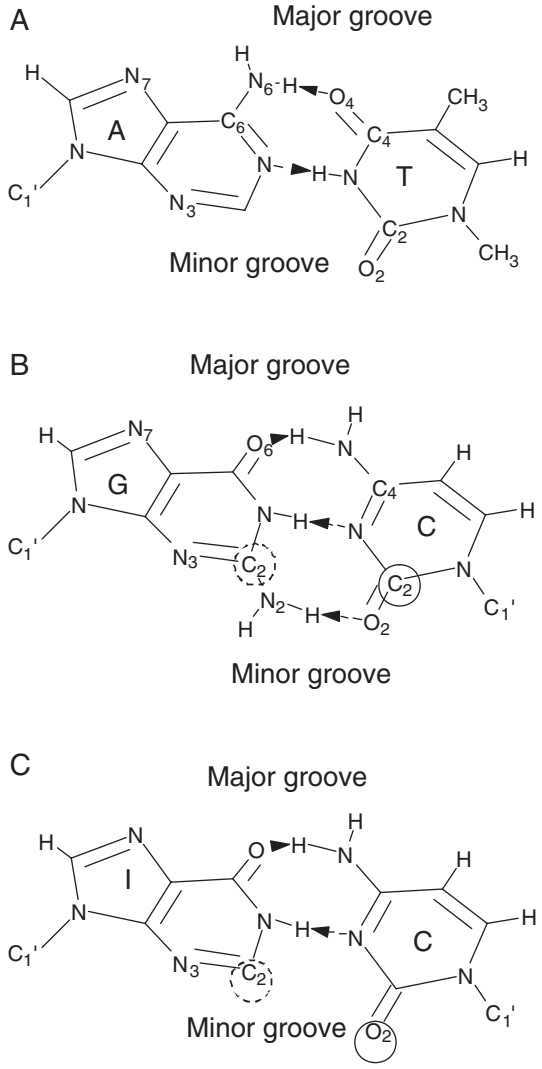

Fig. 1. Structures of (A) A–T, (B) G–C, and (C) I–C base pairs—the missing amine group at C_2 position (dashed circle) can be used to test a potential steric hindrance to spermine binding to the minor groove of G–C base pairs, i.e., to N3 of guanine and O2 of cytosine (full circle).

genomes [15]; the alternate AT sequence (AT/TA motif) is of broad biological significance, illustrated by its function in the regulation of gene transcription in both eukaryotes (TATA box) and prokaryotes (TATAAT, −10 consensus sequence) [16]; GC sequences are known to be hot spots for mutations in DNA—a G→T mutation in a run of seven G's near the 5′ splice site of intron 3 gives rise to the Wiedemann–Beckwith syndrome [17]; telomeres, the end caps of chromosomes, have simple repetitive sequences with one strand G-rich (12–16 bases) relative to the other, C-rich, strand [18,19]. Thus, a systematic study of spermine-induced differential stability of DNA duplexes and associated binding thermodynamics, as a function of nucleotide sequence, may provide insight into the role of spermine in a variety of cellular processes.

Most reports on sequence-dependence of spermine binding to DNA have used small oligomers (hexamers or octamers) [20–23], where base-induced local helix bending can complicate interpretations regarding global secondary structural changes, e.g., B→A transitions [24]. However, recent work probing the structure of DNA within cationic lipid–DNA complexes has utilized 20 bp long oligomers [25]. We have used 20 bp oligomers comprised of (purine:pyrimidine)$_n$ homooligomers and alternate purinepyrimidine oligomers that yield biologically relevant secondary and tertiary structures. They offer the advantage of having two helical turns (~10.2 bp/turn), and hence their overall structure is less dependent on artifacts introduced by base-induced local bending as in shorter oligomers. Thus, sequence-dependent structural changes in DNA as a result of spermine binding, and the corresponding thermodynamic driving forces can be isolated in physiologically relevant structures.

Spermine has been reported to have weak or no base-pair selectivity [26,27] or GC selectivity [28–31] in DNA duplexes. A minor-groove binding site of spermine in AT-rich DNA has been suggested from photoaffinity cleavage studies [32,33]. In mixed sequences spermine binding is diffusive, wherein it shifts between the minor groove of B-DNA (AT rich DNA) and the major groove of A-DNA (G-tracts) [32]. Theoretical studies predict binding of spermine to the major groove of GC-rich duplexes [30,34], and to the minor groove of AT-rich duplexes [35,36]. Potential binding sites for spermine in GC rich DNA are N7 and O6 of guanine in the major groove [37]. We have tested the hypothesis that spermine could bind to N3 of guanine and O2 of cytosine in the minor groove if not for the presence of the guanine N2 amino group (Fig. 1B). According to this hypothesis, inosine–cytosine duplexes should allow binding of spermine to its minor groove, since the IC and GC base pairs differ only by the guanine N2 amino group (Fig. 1C). We test this hypothesis by comparing the energetics of spermine binding to these oligomers by ITC, and monitoring corresponding structural changes by CD. The ability of spermine to induce differential stabilization in polynucleotides has also been studied by thermal melting of the oligonucleotides as a function of spermine concentration. In addition, we address the ability of spermine to discriminate between homooligomers and alternating oligomers by studying secondary and tertiary structure dependent energetics of spermine binding to these sequences.

2. Materials and methods

Single stranded oligonucleotides (20 b)–poly(dA), poly(dT), poly(dG), poly(dC), poly(dAdT), poly(dGdC), and poly(dIdC) – were purchased from Invitrogen Corp. (Carlsbad, CA), in cartridge purified form. The purification process is based on reverse phase chromatography and serves to remove failed sequences after complete synthesis. HEPES (4-(2-Hydroxyethyl)-1-piperazineethane-sulfonic acid), EDTA (ethylenediamine tetra-acetic acid), and spermine tetrachloride were purchased from Sigma Chemical Co. (St. Louis, MO) in powder form and used without further purification.

2.1. Oligonucleotide annealing

Oligonucleotides were solubilized in 5 mM HEPES, 1 mM EDTA, and 150 mM NaCl buffer (pH 6) filtered through a

0.22 μm pore size filter. Concentrations of single stranded oligonucleotides were determined by UV spectroscopy with the aid of extinction coefficients provided by Invitrogen: $\varepsilon_{poly(dA)}=306{,}000\,M^{-1}\ cm^{-1}$, $\varepsilon_{poly(dT)}=186{,}000\,M^{-1}\ cm^{-1}$, $\varepsilon_{poly(dG)}=236{,}000\,M^{-1}\ cm^{-1}$, $\varepsilon_{poly(dC)}=148{,}000\,M^{-1}\ cm^{-1}$, $\varepsilon_{poly(dAdT)}=246{,}000\,M^{-1}\ cm^{-1}$, $\varepsilon_{poly(dGdC)}=192{,}000\,M^{-1}\ cm^{-1}$, and $\varepsilon_{poly(dIdC)}=196{,}500\,M^{-1}\ cm^{-1}$. Concentrations were calculated in moles of single strands — depending on sequence, these values were 10–17% lower than those calculated from the standard nearest neighbor method. The source of these differences lies in the elimination of contributions from nucleotide base stacking to the overall extinction coefficient by Invitrogen. Annealing of homooligomers was carried out by heating equimolar volumes of complementary sequences to 95 °C on a heating block, and by holding them at this temperature for 5 min. The oligonucleotides were allowed to equilibrate to room temperature before being dialyzed overnight at 4 °C with 2 buffer changes of 1 l. Being self-complementary, the alternating polymers were annealed individually. Concentrations of double stranded oligonucleotides were determined by using an average of the extinction coefficients of the individual strands. Molecular sizes of the annealed oligonucleotides were confirmed by polyacrylamide gel electrophoresis by comparison against a 20 bp molecular ladder. All samples had undetectable levels of single strands after annealing.

2.2. Circular dichroism

UV–Vis CD spectra were obtained on an AVIV model 62 DS spectropolarimeter (Lakewood, NJ). Measurements of the samples were taken in a 0.1 cm path length quartz cell and placed in a thermostated cell holder. A double strand molar concentration of 7.5 μM ($[PO_4^{-2}]=0.3$ mM) was used for all oligonucleotides. All spermine solutions were prepared by gravimetry in the final dialysate resulting from oligonucleotide dialysis (see Oligonucleotide annealing). Appropriate volumes from the stock spermine solution were added to achieve different molar ratios; final concentration of spermine varied from 37.5 μM (molar ratio = 5) to 150 μM (molar ratio = 20). Data are presented as the ellipticities per mole of nucleotide phosphate $\varepsilon_L-\varepsilon_R$ ($\Delta\varepsilon$), where ε_L and ε_R are the extinction coefficient for left and right circularly polarized light, respectively.

2.2.1. Wavelength scans

Data were collected at 25 °C, from 350 to 220 nm, at 0.25 nm intervals using a 1.0 nm bandwidth, with an averaging time of 5 s at each point. For AT sequences spectral data points from 350 to 300 nm, and for GC and IC sequences spectral data points from 350 to 320 nm were averaged and used for baseline subtraction. A buffer solution containing the highest concentration of spermine used was scanned to determine absorbance, if any, in the region of interest, i.e., from 300 to 220 nm. No such absorbance was detected.

2.2.2. Temperature scans

Ellipticities of oligonucleotides and their complexes with spermine, at the near UV wavelength of maximum absorption, were monitored as a function of temperature to monitor the transition from double to single stranded oligomers. Samples were heated from 15 to 85 °C at an interval of 1 °C. A heating rate of 1 °C/min was employed, with an equilibration time of 2 min at every temperature. The buffer was heated over the same temperature range and the resulting data used for buffer correction. No difference was observed between absorbance by buffer and that by spermine solution, as a function of temperature. The melting temperatures (T_m) of the oligonucleotides in the absence and presence of spermine were determined by fitting a complex sigmoid model provided with the Igor Pro software (Wavemetrics, Lake Oswego, OR) to the thermal melt data.

The van't Hoff enthalpies of the "premelting" transition [38] in the A–T homooligomer was calculated from the general form of the van't Hoff equation [39]:

$$\Delta H_{vH} = (2+2n)RT_{pm}^2(d\alpha/dT)_{T_{pm}} \quad (1)$$

where n is the molecularity of the transition: $n=1$ since the transition occurs intramolecularly in both duplexes; T_{pm} is the premelting temperature, the mid-point of the premelting transition (at $\alpha=0.5$).

2.3. Isothermal titration calorimetry

2.3.1. Sample preparation

Spermine solutions were prepared by gravimetry and dissolution in the final dialysate obtained from oligonucleotide dialysis. This greatly reduces any differences in the pH and ionic strengths of the ligand and DNA solutions, thus negating any contributions from artifacts arising from buffer–buffer interactions. The sample concentrations used were: 2 mM spermine titrated into 12.5 μM poly(dA):poly(dT), 1 mM spermine titrated into 12.5 μM poly(dG):poly(dC), 1.5 mM spermine titrated into 50 μM poly(dAdT):poly(dAdT), and 2 mM spermine titrated into 37.5 μM poly(dGdC):poly(dGdC). Oligonucleotide concentrations are reported as molar concentrations of double strands. Titrations of poly(dG):poly(dC) with spermine were performed at 3 different oligonucleotide concentrations (7.5, 10 and 12.5 μM), and the error in measurement of ΔH and K_{app} from these samples was not more than the error in these parameters obtained from triplicate measurements at 12.5 μM. The pH values of all spermine and oligonucleotide samples were measured and adjusted to pH 6, if necessary, immediately before the titrations. The choice of this pH for the titrations is based on the observation of heats at higher pH values that are not true representatives of spermine–DNA binding, due to proton transfer between spermine and HEPES buffer. All samples were degassed prior to use, by application of vacuum with simultaneous stirring on a magnetic stir plate.

2.3.2. Instrumentation

An Omega ITC (Microcal, Inc., Northampton, MA) was employed for the calorimetric measurements. Prior to titrations, baseline stability was ascertained by ensuring that the RMS

noise and baseline drift were less than 0.005 and 0.025 μcal/s per 30 min, respectively. For all titrations the DNA solution was held in the sample cell and the reference cell was filled with deionized, filtered and degassed water. In all experiments 18 injections of 15 μl each of spermine, filled in a 250 μl syringe, were made into the 1.32 ml thermally insulated cell filled with oligonucleotide solutions or buffer. In the case of spermine binding to the alternate AT oligomer, the oligomer (held in the syringe) was titrated into spermine (held in the cell), because an adequate binding isotherm could not be obtained when spermine was injected into this oligomer. A stirring speed of 350 rpm was utilized and an interval of 240 s was sufficient between injections for the heat signal to return to the baseline, indicative of system equilibration. Using the same injection parameters the heats of spermine dilution were determined by titration of spermine into buffer; and these heats were subtracted from the heats from spermine–oligomer titrations, to obtain the actual heats of binding.

2.3.3. Data analysis

Origin 2.9 software was used for fitting the Wiseman isotherm for multiple noninteracting sites [40,41],

$$\frac{dq}{dL_T} = \Delta H\left(\frac{1}{2} + \frac{1 - X_R - r}{2\sqrt{(X_R + r + 1)^2 - 4X_R}}\right)V \quad (2)$$

to the calorimetric data by nonlinear least-squares fitting. (dq/dL_T) is the derivative of the heat of binding at a given stage with respect to L_T — the total spermine concentration (mM) injected up to that stage; X_R is the molar ratio of the incremental spermine concentration to the double stranded oligonucleotide concentration (mM) in the cell, i.e., L_T/M_T; $r = 1/(K_b M_T)$; and V is the calorimeter cell volume.

The enthalpy of binding/(mole of spermine) (ΔH) was calculated by normalizing the difference in the heats of binding and dilution to the moles of spermine introduced in each injection, and averaging ΔH values from the initial part of the binding isotherm before the heat of binding begins to decrease, i.e., pretransition ΔH values. The model-free ΔH values thus estimated were used for initialization of the fitting procedure to obtain the apparent binding constant (K_{app}) and the binding stoichiometry (N). The K_{app} is used to calculate the binding free energy change (ΔG) and entropy change (ΔS) of binding by using the following equations:

$$\Delta G = -RT\ln K_{app} \quad (3)$$

$$\Delta S = (\Delta H - \Delta G)/T \quad (4)$$

As shown by Indyk and Fisher [41] the Wiseman isotherm is derived from basic mass action laws, and hence and bears no structural assumptions. More importantly, the dependent variable (dq/dL_T) is not derived, but is directly calculated from the experiment.

3. Results

3.1. Circular dichroism—spermine-induced changes in secondary structure of oligonucleotides

3.1.1. Poly(dA):poly(dT)

The circular dichroism spectrum for double stranded poly (dA):poly(dT) displays positive peaks at 282 and 260 nm, and a negative peak at 247 nm (Fig. 2) [38,42–45]. The 260 nm peak is unusual for the classical B-form DNA, which is characterized by a positive peak at 278 nm and a negative peak at 250 nm in the near UV region [46]. This altered structure of the homooligomer has been shown to be "bent" [47–49]. Upon addition of spermine up to a (spermine/oligo) molar ratio of 20, minimal changes are observed in the intensities of both the 282 and 260 nm bands.

3.1.2. Poly(dAdT):poly(dAdT)

In contrast to the A–T homooligomer the spectra of poly (dAdT):poly(dAdT) exhibits a single positive peak at 268 nm and a negative peak at 247 nm (data not shown), suggestive of the normal B-form DNA. This spectrum is qualitatively consistent with spectra reported for similar sequences in other reports [38,44,45]. A very weak shoulder is observed at 280 nm which is more prominent in the spectra reported by Gennis and Cantor [44] and Greve et al. [45]; this difference might be due to the longer sizes of the oligomers used in their studies. The absence of the 260 nm peak in the alternating AT oligomer, combined with the lack of a bent helix in the crystal structure of these sequences [49] further suggests that this sequence assumes the normal B conformation. There is no detectable change in the overall CD spectrum of poly(dAdT):poly(dAdT) upon addition of spermine, nor does it induce a change in the 268 nm peak intensity (data not shown).

3.1.3. Poly(dG):poly(dC)

Numerous reports on the crystal structures of hexameric and octameric oligonucleotides containing G-tracts have established that these sequences exist in the A-form or a modified A-form [20,21,23,50,51]. The spectra observed for 20 bp poly(dG):poly

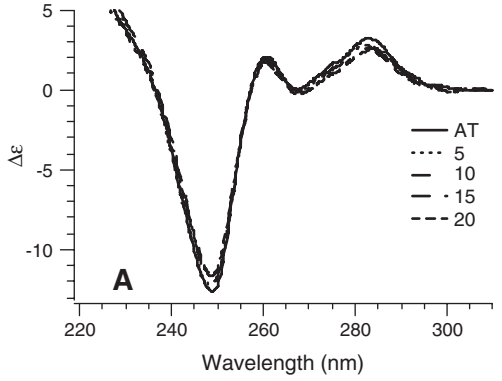

Fig. 2. (A) Circular dichroism spectra of poly(dA):poly(dT) at increasing spermine/oligonucleotide molar ratios. No spermine-induced changes were detected in any of the peak intensities or peak positions for these oligomers.

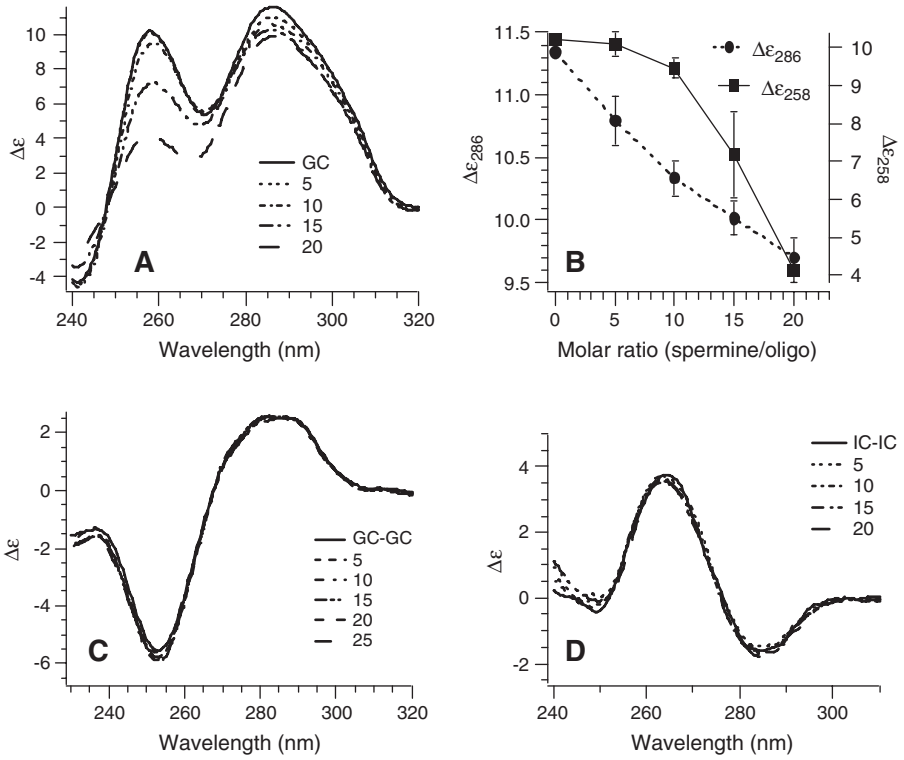

Fig. 3. (A) Circular dichroism spectra of poly(dG):poly(dC) at increasing spermine/oligonucleotide molar ratios. (B) Peak ellipticities at 258 nm (squares) and 286 nm (circles) from poly(dG):poly(dC) profiles in Fig. 3A, at increasing spermine/oligonucleotide molar ratios—spermine induces marked reductions in intensities of both peaks: there is an immediate reduction in the lower wavelength intensity even at the lowest spermine/oligonucleotide molar ratio studied, whereas the 286 nm peak begins to decrease only after charge neutrality (molar ratio = 10; symbols represent average of measurements on 3 different samples, and error bars represent corresponding standard deviations), and (C) CD spectra of poly(dGdC):poly(dGdC) at increasing spermine/oligonucleotide molar ratios, and (D) CD spectra of poly (dIdC):poly(dIdC) at increasing spermine/oligonucleotide molar ratios — no spermine-induced changes were detected in any of the peak intensities or positions for poly(dGdC):poly(dGdC) or poly(dIdC):poly(dIdC).

(dC) (Fig. 3A) show two large positive peaks at 286 and 258 nm. Although embedded G-tracts have a propensity to favor the A-form structure in solution [50–54], the data in Fig. 3A clearly differ from the classical A-form spectra of DNA observed at low water activity [55]. However, it must be remembered that for the data in Fig. 3A, dehydrating conditions, induced either by concentrated salt or ethanolic solutions, were not imposed upon the oligomers; the spectra represent solution structures of the G-tract oligomer in 150 mM NaCl.

The A-form DNA spectrum is characterized by a dramatic increase in the intensity of the longest wavelength transition, accompanied by a blue shift of this peak [56]. In contrast, this peak is red shifted to 286 nm in the spectrum of poly(dG):poly (dC) in our study (Fig. 3A). This is consistent with the spectrum reported for the same oligomer by Braun et al. [25]; although the magnitude of the 286 nm peak is smaller in their report, probably due to the difference in buffer ionic strength. Presumably, a pure G-tract assumes an A/B intermediate secondary structure in vivo. Indeed, there is a correlation between G-tract length and the propensity of DNA to assume the A-form in solution, even though the overall conformation is indicative of the B-form [22]. Interestingly, the appearance of the 286 nm peak was highly correlated with the length of the embedded G-tract, and was dependent on sequence context [22]. The crystal structure of an embedded G-tract in a dodecamer has shown that the central "hole" along the long axis of this strand is larger than that for B-form but smaller than that for A-form DNA [57], further suggesting an A/B intermediate structure for these sequences.

Spermine induces a sharp reduction in both the 286 and 258 nm peak intensities in poly(dG):poly(dC) (Fig. 3B); there is a continuous and linear decrease of the 286 nm peak intensity, whereas the 258 nm signal decreases only at spermine concentrations above that required for charge neutrality ([spermine] = 75 μM; molar ratio 10). The absence of any peak shifts upon addition of spermine (Fig. 3A) suggests that the oligonucleotide maintains its A/B intermediate structure in the presence of spermine.

3.1.4. Poly(dGdC):poly(dGdC)

The alternating GC polymer, like its AT counterpart, exhibits a single positive peak, although red-shifted at 289 nm, and a negative peak at 254 nm, indicative of the B-form (Fig. 3C). The fundamental difference between the G-tract sequence and the alternating GC oligomer spectra – the lack of the 260 nm peak in the latter – reinforces the role of G-tracts in assuming A/B intermediate structures in solution. In agreement with previous reports, addition of spermine induces neither a reduction in peak intensity nor a peak shift in the alternating GC oligomer (Fig. 3C) [58,59].

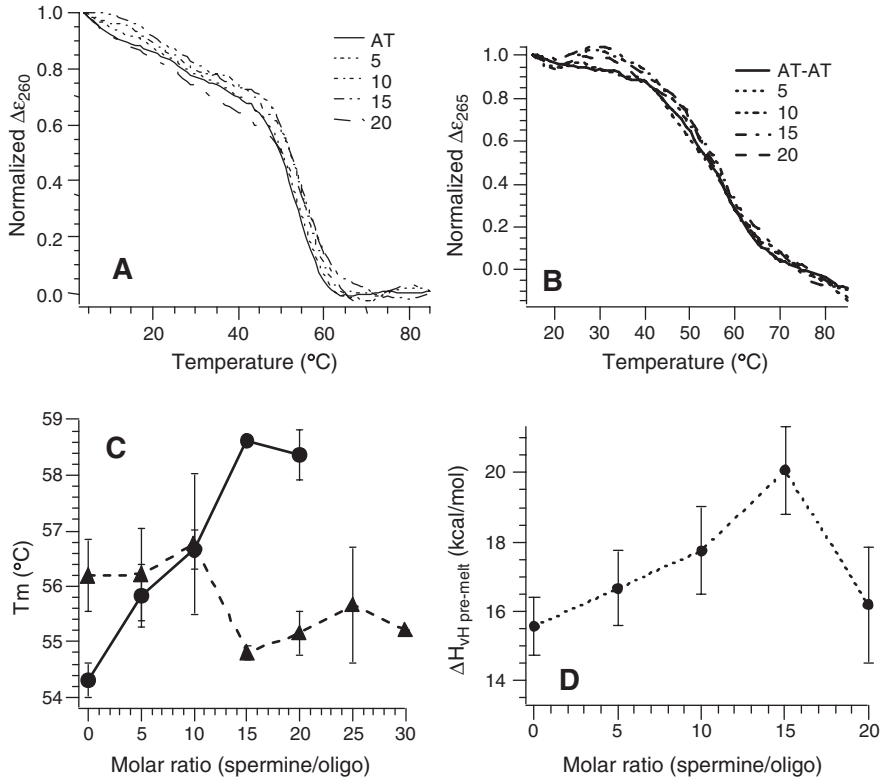

Fig. 4. Normalized thermal melting profiles from temperature-dependent circular dichroism molar ellipticities of (A) poly(dA):poly(dT), and (B) poly(dAdT):poly(dAdT) at increasing spermine/oligonucleotide molar ratios; (C) global melting temperatures (T_ms) of poly(dA):poly(dT) (solid line), and poly(dAdT):poly(dAdT) (dashed line) as a function of spermine/oligonucleotide molar ratio. T_m values are obtained from the mid-points of the curves in (A and B), calculated by fitting the melting profiles to a complex sigmoid function. (D) van't Hoff enthalpies of the "premelting" transition in poly(dA):poly(dT) at increasing spermine/oligonucleotide molar ratios. For C and D — symbols represent average of measurements on 3 different samples, and error bars represent corresponding standard deviations.

3.1.5. Poly(dIdC):poly(dIdC)

There is a small negative peak at 284 nm and a positive peak at 264 nm in the poly(dIdC):poly(dIdC) CD spectrum (Fig. 3D). This spectrum is indicative of the reversed duplex helicity exhibited by the left-handed Z-DNA structure, the difference being that the latter exhibits a much larger negative peak at 292 nm and a positive peak at 270 nm [60,61]. Studies have also shown that the intensity of the 292 nm peak decreases in the presence of 85% ethanol, and the resultant spectrum closely resembles that of the alternate IC oligomer in magnitude — this dehydrated structure is called the Z′ form of DNA. However, both major peaks are red-shifted by ~10 nm in the Z′-form compared to the alternating IC polymer. There is no change in the CD spectrum of this oligomer upon addition of spermine.

3.2. Circular dichroism—thermal stability induced by spermine in oligonucleotides

3.2.1. Poly(dA):poly(dT)

The 260 nm CD band is lost upon thermal melting of the A–T homooligomer in 150 mM NaCl, and the intensity of this band is used as an indicator of the fraction of double stranded poly (dA):poly(dT). Fig. 4A reveals that between 4 and 45 °C there is a broad pretransition in the 260 nm band intensity, with a transition midpoint at 25 °C. This change has been referred to as the "premelting" phase in previous CD [38,62] and Raman spectroscopy studies [63–65]. The presence of an isosbestic point (two state transition) in the premelting phase of the A–T homopolymer (data not shown) [38] allows estimation of the apparent van't Hoff enthalpy (ΔH_{vH}) of premelting (see Materials and methods). The calculated ΔH_{vH} of poly(dA):poly(dT), 15.56 ± 0.84 kcal/mol per cooperative unit, is within the error of that reported by Dickerson et al. (20.5 ± 5.0 kcal/mol) [37], but lower than that measured by Herrera and Chaires (19.9 kcal/mol) [62]. A variability of measurement was not reported in the latter study, which makes comparison difficult. The ΔH_{vH} of premelting increases in magnitude with increasing spermine concentration; this trend continues up to a molar ratio (spermine/oligo) of 15 (ΔH_{vH} = 20.06 ± 1.28 kcal/mol) and decreases again at 20 (Fig. 4D). However, there is no corresponding increase in the transition midpoint of the premelting phase.

The melting temperature of the 20 bp A–T homooligomer in 150 mM NaCl is measured to be 54.31 ± 0.3 °C. This value represents a global melting resulting from double to single strand transition, i.e., disruption of the Watson–Crick H-bonding. There is a linear increase in the T_m of poly(dA):poly(dT) with increasing spermine concentrations, until at a (spermine/oligo) molar ratio of 20 ([spermine] = 150 μM) the T_m reaches 58.37 ± 1.86. Thus, spermine induces an increase in the canonical T_m of poly(dA):poly(dT) by >4 °C (Fig. 4C).

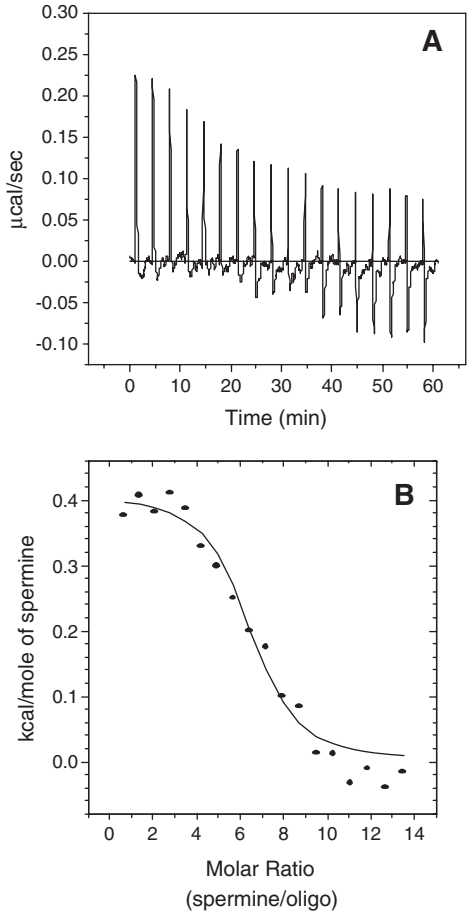

Fig. 5. (A) Raw, unsubtracted calorimetric binding heats obtained from titration of spermine into poly(dG):poly(dC)—horizontal solid line at zero represents the baseline. The positive (endothermic) heats in the first phase of the titration represent spermine–oligomer binding heats, which decrease in magnitude as binding sites on the oligomer are saturated. The predominantly negative (exothermic) heats in the second phase of the titration represent the spermine heat of dilution. Subtraction of the heats of dilution (obtained from separate titrations) from the complete titration curve yields the actual binding isotherm reported in 6B. (B) Spermine–poly(dG):poly(dC) binding isotherm constructed by normalizing the heats of binding to the moles of spermine injected.

3.2.2. Poly(dAdT):poly(dAdT)

For the alternating AT oligomer, the intensity of the 265 nm peak was monitored as a function of temperature to follow the double to single strand transition. Unlike the melting profiles for the A-tract homooligomer, the alternating AT oligomer does not display a premelting phase (Fig. 4B); with a T_m for ds→ss transition of 56.2±0.65 °C. There is no spermine-induced stabilization of the double stranded form of the alternate AT oligomer. In fact, above molar ratio 10 the T_m decreases by ~1.5 to 55 °C and remains relatively unchanged until molar ratio 30 (Fig. 4C).

3.2.3. Poly(dG):poly(dC)

Under the present buffer conditions the 20 bp GC homo-oligomer displays a T_m of 54.4±1.3 °C (melting curves not shown). It must be noted that this sequence did not display any thermal melting event at pH 7.4 (data not shown), indicating that the stability of this sequence might be compromised by the incumbent pH, 6. Indeed, the N3 in cytidine has a pK_a of ~4.2 [66]. Thus, even though no single stranded species or larger assemblies (triplexes or quadruplexes) were observed by polyacrylamide gel electrophoresis, a charged cytidine fraction of 0.016 (calculated from the Henderson Hasselbalch equation) might contribute to the observed low T_m for this sequence. There is no significant change in the T_m of this sequence in the presence of spermine.

Melting temperatures could not be calculated for the alternating GC and IC sequences in 150 mM NaCl due to the absence of a transition in their CD signals up to 90 °C.

3.3. Isothermal titration calorimetry

Fig. 5A shows representative binding heats obtained from titration of spermine into poly(dG):poly(dC). Two observations in the binding isotherm are apparent: (i) the positive heats indicate that binding is enthalpically unfavorable (Table 1), and (ii) the resultant sigmoid binding profile (Fig. 5B) lacks a second endothermic peak that has been associated with plasmid DNA collapse and condensation induced by cobalt hexamine, spermidine [67], and spermine [68] binding. Indeed, DNA molecules longer than 400 bp are necessary to stabilize the condensed particles [69,70]. The absence of the formation of spermine-induced multimolecular assemblies was confirmed by dynamic light scattering (data not shown). The binding curve characteristics described above are observed in the isotherms for spermine binding to all oligonucleotide sequences studied (curves not shown).

The enthalpies of spermine binding to all sequences except poly(dIdC):poly(dIdC) are quite similar (Table 1). With the exception of poly(dIdC):poly(dIdC) the binding free energies (ΔG) for all other sequences are driven only by favorable

Table 1
Thermodynamic parameters for binding of spermine to different DNA oligomeric duplexes

	Poly(dG):poly(dC)	Poly(dA):poly(dT)	Poly(dGdC):poly(dGdC)	*Poly(dAdT):poly(dAdT)	Poly(dIdC):poly(dIdC)
ΔH (cal/mol)	445.23±43.23	397±97.43	442.3±20.5	399.25±45.7	−338±146.32
ΔS (cal/mol K)	24.86±1.16	21.98±0.11	22.1±1.16	32.12±1.8	
ΔG (cal/mol)	−6964±388.6	−6153.04±63.72	−6143.5±325.07	−6900±297	
K_{app} (M^{-1})	1.46e5±8.1e4	3.24e4±3.75e3	3.45e4±1.81e4	1.16e5±3.5e4	
N	5.69±0.88	5.89±2.49	6.58±0.28	6.7±1.2	

N=binding stoichiometry defined as molar ratio [spermine]/[ds-oligonucleotide].
n=3.
* Binding enthalpy calculated from titration of poly(dAdT):poly(dAdT) into spermine.

entropies. A complete binding isotherm could not be obtained for spermine–poly(dIdC):poly(dIdC) binding; hence only a ΔH of binding could be calculated. Interestingly, spermine binds to this sequence with a favorable enthalpy that is comparable in magnitude to the endothermic ΔH values calculated for spermine binding to the other sequences (Table 1). The estimated apparent binding constants (K_{app}) for spermine binding to poly(dG):poly(dC) and poly(dAdT):poly(dAdT) are similar, and an order of magnitude higher than those for spermine binding to poly(dA):poly(dT) and poly(dGdC):poly (dGdC).

There are no significant differences between the calculated binding stoichiometries (N) for all sequences. It must be noted that the N values are reported in units of [spermine]/[ds-oligonucleotide] (molar ratio), and must be divided by 10 in order to obtain the (NH_4^+/PO_4^-) charge ratio. Thus, the data suggest that at saturation only approximately half of the oligonucleotide phosphates are bound by spermine molecules.

4. Discussion

4.1. Preferential stabilization of poly(dA):poly(dT)

In agreement with previous studies, CD thermal melting profiles show that A-tracts undergo a premelting conformational transition [38,63,64]. The melting profiles show that between 4 and 45 °C there is an ~40% noncooperative loss in the 260 nm signal, which is likely due to thermally induced reduction in base stacking (π–π interactions) [46]. The noncooperativity of this transition indicates that it does not arise from disruption of interstrand hydrogen bonds, i.e., ds → ss transition.

The unusual conformation exhibited by A-tracts in solution is responsible for DNA bending, which is induced by a narrow minor groove, a major groove that is wider than that in B-form DNA [47–49,70,71]. This creates an additional, bifurcated H-bond between N6 of adenine and O4 of the adjacent thymine on the 3′ side (Fig. 1), i.e., diagonally across the major groove [48,72–74]. The calculated premelting van't Hoff enthalpy (ΔH_{vH}), assuming a two state transition, is 15.56 ± 0.84 kcal/mol per cooperative unit, and increases with spermine concentration until a molar ratio of 15. The modified conformation of the A-tract oligomer might be disrupted as the temperature is raised towards the global melting temperature, driving the oligonucleotide strand to assume the B-form structure [62]. Although the initial increase in the pre-melting ΔH_{vH} suggests that spermine imparts thermostability to the bent conformation of A-tracts, this idea must be qualified due to the subsequent decrease of ΔH_{vH} at molar ratio 20. This decrease cannot be reconciled with a simple two-state model. Moreover, there is no corresponding increase in the pretransition midpoint (plot not shown), further qualifying any interpretations regarding stabilization of bent form of A-tracts by spermine.

In the presence of spermine the T_m calculated from the cooperative phase of the melting profiles, that represent double to single strand transition, increases by >4 °C, indicating that spermine stabilizes the double stranded form of A-tracts. Indeed, a preferential interaction of spermine with bent A-tracts embedded in ds-DNA has been established [33]; however, spermine-induced preferential thermal stabilization of double stranded A-tract oligomers has not been reported earlier. No such stabilization is observed for any of the other sequences studied, including the alternate AT oligomer. Thus, the bent structure of A-tract DNA might play a crucial role in its preferential stabilization by spermine. That spermine-induced changes in strand flexibility do not compromise this interpretation is supported by the minimal change in helicity of this sequence upon spermine binding (Fig. 2). Moreover, we can also rule out strand compaction/condensation or intermolecular interactions at higher spermine concentrations, on account of absence of any change in the hydrodynamic radius of this oligomer (data not shown); consistent with the inability of DNA strands <400 bp to undergo compaction [69,70]. The decrease in T_m of the alternate AT oligomer above charge neutrality is contradictory to numerous reports on multivalent cation-induced DNA stabilization. In any case, the magnitude of this change (~1.5 °C) is within the error of measurement of most samples; hence we do not attribute any physical meaning to these changes.

That base-specific binding plays a role in the selective stabilization of A-tracts by spermine seems unlikely when it is considered that the ΔG of spermine–poly(dA):poly(dT) binding is driven solely by a favorable entropy change (Table 1). It is important to remember that such sequences are highly hydrated and possess an ordered "spine of hydration" in the minor groove [47,75,76]. The bound water molecules forming the "spine of hydration" exhibit much slower exchange rates with bulk solvent than those bound to other sequences [77,78], and its disruption would be a prerequisite for base-binding of spermine. Such a displacement of water from A-tract sequences is indicated by binding of dimethyl sulfoxide, which induces the same conformational change in poly(dA):poly(dT), as monitored by circular dichroism, that is observed at higher temperatures, i.e., loss of the 260 nm peak [62]. Clearly, such a change in the CD spectra of the A-tract sequence does not occur upon spermine binding (Fig. 2). This suggests that the favorable entropy of binding does not arise from displacement by spermine of water bound to the minor groove of A-tracts. This is supported by the lower ΔS measured for spermine binding to this sequence, compared to that to other oligomers (Table 1). So, we propose that preferential stabilization of A-tract DNA by spermine does not arise predominantly from base-specific binding of spermine to these sequences. One of the possibilities might be that the bent structure of A-tracts makes it more favorable for spermine to bind phosphates on both strands of DNA by spanning the grooves. This could impart preferential stabilization upon the double stranded form of A-tract DNA over other sequences.

Although spermine binding to the major groove of GC-rich sequences has been previously reported [30,59], the endothermic ΔH of spermine binding to both GC sequences does not support this interpretation (Table 1). The absence of the N2 group of guanine in the minor groove of the IC oligomer was used to test the hypothesis that this group poses a hindrance to spermine binding in the minor groove of GC oligomers.

Although binding of spermine to the IC oligomer proceeds with a favorable ΔH (-338 ± 146.32), it must be remembered that its Z′-form structure (Fig. 3D) might play a role in this different mode of binding compared to that of spermine binding to the alternating GC oligomer, which exhibits the B-form structure in 150 mM NaCl (Fig. 3C).

4.2. Implications for DNA condensation and nucleosome stability

The physical behavior of polynucleotides is an interesting subject on its own accord, but it acquires increased significance when it impinges on the understanding of DNA packaging for gene delivery applications and for regulatory processes in the cell. This study shows that at physiologically relevant NaCl and spermine concentrations, the latter is able to differentially stabilize polynucleotides based on sequence; and this ability is translated from the primary to the secondary–differential changes in helical flexibilities in homooligomers compared to the alternate oligomers–to the tertiary structural level—preferential stabilization of A-tracts.

Reconstitution studies have shown that nucleosomes are destabilized by long regions of polynucleotides that substantially deviate from the B-form of DNA; thus, it is not surprising that A-tract and G-tract phases in genomic DNA resist formation of stable nucleosomes when challenged by histones [79]. Intrinsically bent A-tract phases are characterized by substantially attenuated affinities toward DNA-binding proteins involved in structural functions, such as H1 histone (chromatin) and protamine (sperm cells) [80]. Indeed, they can be incorporated into nucleosomes only at higher temperatures [81] where they are rendered more flexible as their inherent curvature is lost by disruption of the spine of hydration. Even though ITC data suggest a lower affinity for spermine binding to A-tracts compared with other sequences, the CD thermal melting data demonstrate a stabilizing effect on A-tracts by spermine. We speculate that the inability of spermine to eliminate strand curvature in A-tracts, rather an induction of selective stabilization, has implications for polyamines in stabilization of such phases in non-nucleosomal structures. Indeed, A-tract runs of 20 bp are preferentially positioned at the ends of the nucleosome core [82]. By stabilizing A-tracts over other sequences, spermine could potentially modulate protein–nucleic acid interactions that are DNA sequence-dependent. For example, it is known that spermine induces a high level of positive stress in the pre-transcribed phase of T7 DNA, which enhances its transcriptional activity [83]. Induction of positive stress is a direct function of decrease in DNA flexibility or rotational freedom, which in turn arises from DNA bending. In light of the data reported in the current study, i.e., stabilization by spermine of A-tracts (at physiological ionic strength), it would follow that physiological concentrations of spermine (1–2 mM) could promote transcription of A-tracts by decreasing their flexibility in closed circular DNA.

In order for topoisomerases to be able to relieve the positive stress in prokaryotic DNA, single stranded character in DNA must be produced by helical distortions or increased flexibility. Our data suggest that the ability of spermine to affect DNA flexibility is sequence-dependent—the higher binding affinity of spermine to G-tracts is accompanied by a reduction in base stacking or helicity (Fig. 3A + B), thereby rendering such phases more flexible and providing a possible compensating mechanism for stabilizing G-tract phases in nucleosomes. This is supported by the higher entropy change measured for spermine binding to G-tracts than to A-tracts or the alternate sequence oligomers (Table 1). This differential induction of structural changes by spermine in duplex oligomers presumably arises from varying sequence-dependent hydration levels—the absence of any spermine-induced changes in secondary structures of the alternate GC and AT oligomers correlates well with their stronger hydration [84,85].

5. Conclusions

This study demonstrates that the ability of spermine to differentiate between polynucleotides based on sequence is translated to physiologically relevant secondary and tertiary nucleic acid structures assumed by (purine:pyrimidine)$_n$ homooligomers and alternate (purine–pyrimidine)$_n$ oligomers. It is evident that spermine preferentially stabilizes the double stranded form of A-tracts. Spermine also selectively increases flexibility of double stranded G-tract oligomers, as well as exhibits a stronger binding affinity to this sequence and to the alternate AT oligomer, than to the AT homooligomer and the alternate GC oligomer.

Acknowledgements

We are grateful to Dr. Mair Churchill (University of Colorado Health Sciences Center) for her valuable suggestions regarding the use of the inosine oligomers in this study; and to Dr. Brian Lobo (Genentech, San Francisco, CA) for his insight regarding ITC data. We also acknowledge funding from NSF Bioengineering grant # BES-0433811 to TJA.

References

[1] A.C. Childs, D.J. Mehta, E.W. Gerner, Polyamine-dependent gene expression, Cell. Mol. Life Sci. 60 (2003) 1394–1406.
[2] S.S. Cohen, Introduction of the Polyamines, Prentice-Hall, Englewood Cliffs, NJ, 1971.
[3] S.S. Cohen, A Guide to Polyamines, Oxford University Press, New York, NY, 1998.
[4] C.W. Tabor, H. Tabor, Polyamines, Ann. Rev. Biochem. 53 (1984) 749–790.
[5] S. Watanabe, K. Kusama-Eguchi, H. Kobayashi, K. Igarashi, Estimation of polyamine binding to macromolecules and ATP in bovine lymphocytes and rat liver, J. Biol. Chem. 266 (1991) 20803–20809.
[6] K. Igarashi, K. Kashiwagi, Polyamines: mysterious modulators of cellular functions, Biochem. Biophys. Res. Commun. 271 (2000) 559–564.
[7] H.H. Chen, M.J. Behe, D.C. Rau, Critical amount of oligovalent ion binding required for the B–Z transition of poly (dG-m5dC), Nucleic Acids Res. 12 (1984) 2381–2389.
[8] T.J. Thomas, R.P. Messner, A left-handed (Z) conformation of poly(dA-C). poly(dG-dT) induced by polyamines, Nucleic Acids Res. 14 (1986) 6721–6733.

[9] M. Egli, L.D. Williams, Q. Gao, A. Rich, Structure of the pure-spermine form of Z-DNA (magnesium free) at 1-A resolution, Biochemistry 30 (1991) 11388–11402.
[10] T.J. Thomas, V.A. Bloomfield, Ionic and structural effects on the thermal helix–coil transition of DNA complexed with natural and synthetic polyamines, Biopolymers 23 (1984) 1295–1306.
[11] D.M. Hougaard, L. Bolund, K. Fujiwara, L.-J. Larsson, Endogenous polyamines are intimately associated with highly condensed chromatin in vivo. A fluorescence cytochemical and immunocytochemical study of spermine and spermidine during the cell cycle and in reactivated nuclei, Eur. J. Cell Biol. 44 (1987) 151–155.
[12] I.V. Smirnov, S.I. Dimitrov, V.L. Makarov, Polyamine–DNA interactions. Condensation of chromatin and naked DNA, J. Biomol. Struct. Dyn. 5 (1988) 1149–1161.
[13] G. Kolata, New clues to gene regulation, Science 224 (1984) 588–589.
[14] M. Behe, The DNA sequence of the human β-globin region is strongly biased in favor of long strings of contiguous purine or pyrimidine residues, Biochemistry 26 (1987) 7870–7875.
[15] S. Karlin, B.E. Blaisdell, R.J. Sapolsky, L. Cardon, C. Burge, Assessments of DNA inhomogeneities in yeast chromosome III, Nucleic Acids Res. 21 (1993) 703–711.
[16] R.K. Alleman, M., Egli, DNA recognition and bending, Chem. Biol. 4 (1997) 643–650.
[17] J.M. Lew, Y.L. Fei, K. Aleck, B.J. Blencowe, R. Weksberg, P.D. Sadowski, CDKN1C mutation in Wiedemann–Beckwith syndrome patients reduces RNA splicing efficiency and identifies a splicing enhancer, Am. J. Med. Genet. A 127 (2004) 268–276.
[18] C.C. Hardin, E. Henderson, T. Watson, J.K. Prosser, Monovalent cation-induced structural transitions in telomeric DNAs: G-DNA folding intermediates, Biochemistry 30 (1991) 4460–4472.
[19] S. Ahmed, E. Henderson, Formation of novel hairpin structures by telomeric C-strand oligonucleotides, Nucleic Acids Res. 20 (1992) 507–511.
[20] S. Jain, G. Zon, M. Sundaralingam, Base only binding of spermine in the deep groove of the A-DNA octamer d(GTGTACAC), Biochemistry 28 (1989) 2360–2364.
[21] Q. Xu, R.K. Shoemaker, W.H. Braunlin, Induction of B–A transitions of deoxyoligonucleotides by multivalent cations in dilute aqueous solution, Biophys. J. 65 (1993) 1039–1049.
[22] M. Lindqvist, A. Gräslund, An FTIR and CD study of the structural effects of G-tract length and sequence context on DNA conformation in solution, J. Mol. Biol. 314 (2001) 423–432.
[23] J.M. Vargason, K. Henderson, P.S. Ho, A crystallographic map of the transition from B-DNA to A-DNA, Proc. Natl. Acad. Sci. U. S. A. 98 (2001) 7265–7270.
[24] R.E. Dickerson, H.L. Ng, DNA structure from A to B, Proc. Natl. Acad. Sci. U. S. A. 98 (2001) 6986–6988.
[25] C.S. Braun, G.S. Jas, S. Choosakoonkriang, G.S. Koe, J.G. Smith, C.R. Middaugh, The structure of DNA within cationic lipid/DNA complexes, Biophys. J. 84 (2003) 1114–1123.
[26] S. Hirschman, M. Leng, G. Felsenfield, Interaction of spermine and DNA, Biopolymers 5 (1967) 227–233.
[27] J.E. Morgan, J.W. Blankenship, H.R. Matthews, Association constants for the interaction of double-stranded and single-stranded DNA with spermine, spermidine, putrescine, diaminopropane, N1- and N8-acetylspermidine, and magnesium: determination from analysis of the broadening of thermal denaturation curves, Arch. Biochem. Biophys. 246 (1986) 225–232.
[28] K. Igarashi, I. Sakamoto, N. Goto, K. Kashiwagi, R. Honma, S. Hirose, Interaction between polyamines and nucleic acids or phospholipids, Arch. Biochem. Biophys. 219 (1982) 438–443.
[29] K.D. Stewart, The effect of structural changes in a polyamine backbone on its DNA-binding properties, Biochem. Biophys. Res. Commun. 152 (1988) 1441–1446.
[30] M. Yuki, V. Grukhin, C.-S. Lee, I.S. Haworth, Spermine binding to GC-rich DNA: experimental and theoretical studies, Arch. Biochem. Biophys. 325 (1996) 39–46.
[31] H. Deng, V.A. Bloomfield, J.M. Benevides, G.J. Thomas Jr., Structural basis of polyamine-DNA recognition: spermidine and spermine interactions with genomic B-DNAs of different GC content probed by Raman spectroscopy, Nucleic Acids Res. 28 (2000) 3379–3385.
[32] N. Schmid, J.P. Behr, Location of spermine and other polyamines on DNA as revealed by photoaffinity cleavage with polyaminobenzenediazonium salts, Biochemistry 30 (1991) 4357–4361.
[33] S. Lindemose, P.E. Nielsen, N.E. Møllegaard, Polyamines preferentially interact with bent adenine tracts in double-stranded DNA, Nucleic Acids Res. 33 (2005) 1709–1803.
[34] B.G. Feuerstein, N. Pattabiraman, L.J. Marton, Molecular mechanics of the interactions of spermine with DNA: DNA bending as a result of ligand binding, Nucleic Acids Res. 18 (1990) 1271–1282.
[35] B.G. Feuerstein, N. Pattabiraman, L.J. Marton, Spermine–DNA interactions: a theoretical study, Proc. Natl. Acad. Sci. U. S. A. 83 (1986) 5948–5952.
[36] K. Zakrzewska, B. Pullman, Spermine–nucleic acid interactions: a theoretical study, Biopolymers 25 (1986) 375–392.
[37] R.E. Dickerson, M.L. Kopka, P.E. Pjura, NATO ASI Ser., A 137 (1987) 45–62.
[38] S.S. Chan, K.J. Breslauer, M.E. Hogan, D.J. Kessler, R.H. Austin, J. Ojemann, J.M. Passner, N.C. Wiles, Physical studies of DNA premelting equilibria in duplexes with and without homo dA.dT tracts: correlations with DNA bending, Biochemistry 29 (1990) 6161–6171.
[39] C.R. Cantor, P.R. Schimmel, Biophysical Chemistry Part II, Freeman, CA, 1980, p. 384.
[40] T. Wiseman, S. Williston, J.F. Brands, L.-N. Lin, Rapid measurement of binding constants and heats of binding using a new titration calorimeter, Anal. Biochem. 179 (1989) 131–137.
[41] L. Indyk, H.F. Fisher, Theoretical aspects of isothermal titration calorimetry, Methods Enzymol. 295 (1998) 350–364.
[42] J. Brahms, W.F.H.M. Mommerts, A study of conformation of nucleic acids in solution by means of circular dichroism, J. Mol. Biol. 10 (1964) 73–88.
[43] R.D. Wells, J.E. Larson, R.C. Grant, B.E. Shortle, C.R. Cantor, Physicochemical studies on polydeoxyribonucleotides containing defined repeating nucleotide sequences, J. Mol. Biol. 54 (1970) 465–497.
[44] R.B. Gennis, C.R. Cantor, Optical studies of a conformational change in DNA before melting, J. Mol. Biol. 65 (1972) 381–399.
[45] J. Greve, M.F. Maestre, A. Leving, Circular dichroism of adenine and thymine containing synthetic polynucleotides, Biopolymers 16 (1977) 1489–1504.
[46] G.D. Fasman, Circular Dichroism and the Conformational Analysis of Biomolecules, Plenum Press, New York, 1996.
[47] D.G. Alexeev, A.A. Lipanov, I.Ya. Skuratovskii, Poly(dA).poly(dT) is a B-type double helix with a distinctively narrow minor groove, Nature 325 (1987) 821–823.
[48] H.C.M. Nelson, J.T. Finch, B.F. Luisi, A. Klug, The structure of an oligo (dA).oligo(dT) tract and its biological implications, Nature 330 (1987) 221–226.
[49] R. Chandrasekaran, A. Radha, Structure of poly d(A).poly d(T), J. Biomol. Struct. Dyn. 10 (1992) 153–168.
[50] A.H. Wang, S. Fujii, J.H. van Boom, A. Rich, Molecular structure of the octamer d(G-G-C-C-GG- C-C): modified A-DNA, Proc. Natl. Acad. Sci. U. S. A. 79 (1982) 3968–3972.
[51] B.H. Mooers, G.P. Schroth, W.W. Baxter, P.S. Ho, Alternating and non-alternating dG–dC hexanucleotides crystallize as canonical A-DNA, J. Mol. Biol. 249 (1995) 772–784.
[52] V.I. Ivanov, L.E. Minchenkova, E.E. Minyat, M.D. Frank-Kamenetskii, A. K. Schyolkina, The *B* to A transition of DNA in solution, J. Mol. Biol. 87 (1974) 817–833.
[53] T.E. Cheatham III, J. Srinivasan, D.A. Case, P.A. Kollman, Molecular dynamics and continuum solvent studies of the stability of polyG–polyC and polyA–polyT DNA duplexes in solution, J. Biomol. Struct. Dyn. 16 (1998) 265–280.
[54] Y.-G. Gao, H. Robinson, A.H.-J. Wang, High-resolution A-DNA crystal structures of d(AGGGGCCCCT)—an A-DNA model of poly(dG)·poly (dC), Eur. J. Biochem. 261 (1999) 413–420.
[55] J.C. Girod, W.C. Johnson Jr., S.K. Huntington, M.F. Maestre, Conformation of deoxyribonucleic acid in alcohol solutions, Biochemistry 12 (1973) 5092–5096.

[56] J.H. Riazance, W.A. Baase, W.C. Johnson Jr., K. Hall, P. Cruz, I. Tinoco Jr., Evidence for Z-form RNA by vacuum UV circular dichroism, Nucleic Acids Res. 13 (1985) 4983–4989.
[57] H.-L. Ng, M.L. Kopka, R.E. Dickerson, The structure of a stable intermediate in the A↔B DNA helix transition, Proc. Natl. Acad. Sci. U. S. A. 97 (2000) 2035–2039.
[58] J. Nickol, M. Behe, G. Felsenfeld, Effect of the B–Z transition in poly(dG-m5dC). poly(dGm5dC) on nucleosome formation, Proc. Natl. Acad. Sci. U. S. A. 79 (1982) 1771–1774.
[59] R. Marquet, C. Houssier, Different binding modes of spermine to A–T and G–C base pairs modulate the bending and stiffening of the DNA double helix, J. Biomol. Struct. Dyn. 6 (1988) 235–246.
[60] K.B. Hall, M.F. Maestre, Temperature-dependent reversible transition of poly(dCdG):poly(dCdG) in ethanolic and methanolic solutions, Biopolymers 23 (1984) 2127–2139.
[61] M.E. Harder, W.C. Johnson Jr., Stabilization of the Z′-form of poly (dGdC):poly(dGdC) in solution by multivalent ions relates to the Z_{II} form in crystals, Nucleic Acids Res. 18 (1990) 2141–2148.
[62] J.E. Herrera, J.B. Chaires, A premelting conformational transition in poly (dA):poly(dT) coupled to daunomycin binding, Biochemistry 28 (1989) 1993–2000.
[63] S.S. Chan, R.H. Austin, I. Mukerji, T.G. Spiro, Temperature-dependent ultraviolet resonance Raman spectroscopy of the premelting state of dA·dT DNA, Biophys. J. 72 (1997) 1512–1520.
[64] L. Movileanu, J.M. Benevides, G.J. Thomas Jr., Temperature dependence of the Raman spectrum of DNA: II. Raman signatures of premelting and melting transitions of poly(dA):poly(dT) and comparison with poly (dA5dT):poly(dA–dT), Biopolymers 63 (2002) 181–194.
[65] L. Movileanu, J.M. Benevides, G.J. Thomas Jr., Determination of base and backbone contributions to the thermodynamics of premelting and melting transitions in *B* DNA, Nucleic Acids Res. 30 (2002) 3767–3777.
[66] V.A. Bloomfield, D.M. Crothers, I. Tinoco Jr., Nucleic Acids—Structures, Properties, and Functions, University Science Books, Sausalito, CA, 2000, p. 29.
[67] D. Matulis, I. Rouzina, V.A. Bloomfield, Thermodynamics of DNA binding and condensation: isothermal calorimetry and electrostatic mechanism, J. Mol. Biol. 296 (2000) 1053–1063.
[68] M.M. Patel, T.J. Anchordoquy, Contribution of hydrophobicity to thermodynamics of ligand–DNA binding and DNA collapse, Biophys. J. 88 (2005) 2089–2103.
[69] J. Widom, R.L. Baldwin, Cation-induced toroidal condensation of DNA studies with $Co^{3+}(NH_3)_6$, J. Mol. Biol. 144 (1980) 431–453.
[70] R. Marquet, A. Wyart, C. Houssier, Influence of DNA length on spermine-induced condensation. Importance of the bending and stiffening of DNA, Biochim. Biophys. Acta 909 (1987) 165–172.
[71] H.M. Wu, D.M. Crothers, The locus of sequence-directed and protein-induced DNA bending, Nature 308 (1984) 509–513.
[72] W.K. Olson, M.H. Sarma, R.H. Sarma, M. Sundaralingam (Eds.), Structure and Expression Volume 3: DNA Bending and Curvature, Adenine Press, Schenectady, NY, 1988.
[73] C. Yoon, G.G. Prive, D.S. Goodsell, R.E. Dickerson, Structure of an alternating B-DNA helix and its relationship to A-tract DNA, Proc. Natl. Acad. Sci. U. S. A. 85 (1988) 6332–6336.
[74] J. Aymami, M. Coll, C.A. Frederick, A.H.-J. Wang, A. Rich, The propeller DNA conformation of poly(dA) · poly(dT), Nucleic Acids Res. 17 (1989) 3229–3245.
[75] V.A. Buckin, B.I. Kankiya, N.V. Bulichov, A.V. Lebedev, I.Ya. Gukovsky, V.P. Chuprina, A.P. Sarvazyan, A.R. Williams, Measurement of anomalously high hydration of $(dA)_n \cdot (dT)_n$ double helices in dilute solution, Nature 340 (1989) 321–322.
[76] X. Shui, L. McFail-Isom, G.G. Hu, L.D. Williams, The B-DNA dodecamer at high resolution reveals a spine of water on sodium, Biochemistry 37 (1998) 8341–8355.
[77] E. Liepinsh, G. Otting, K. Wuthrich, NMR observation of individual molecules of hydration water bound to DNA duplexes: direct evidence for a spine of hydration water present in aqueous solution, Nucleic Acids Res. 20 (1992) 6549–6553.
[78] B. Halle, V.P. Denisov, Water and monovalent ions in the minor groove of B-DNA oligonucleotides as seen by NMR, Biopolymers 48 (1998) 210–233.
[79] J.D. McGhee, G. Felsenfeld, Nucleosome structure, Ann. Rev. Biochem. 49 (1980) 1115–11156.
[80] M. Shatzky-Schwartz, Y. Hiller, Z. Reich, R. Ghirlando, S. Weinberger, A. Minsky, Attenuation of DNA–protein interactions associated with intrinsic, sequence-dependent DNA curvature, Biochemistry 31 (1992) 2339–2346.
[81] H.L. Puhl, M.J. Behe, Poly(dA)·poly(dT) forms very stable nucleosomes at higher temperatures, J. Mol. Biol. 245 (1995) 559–567.
[82] A. Prunell, Nucleosome reconstitution on plasmid-inserted poly(dA).poly (dT), EMBO J. 1 (1982) 173–179.
[83] H.F. Peng, V. Jackson, In vitro studies on the maintenance of transcription-induced stress by histones and polyamines, J. Biol. Chem. 275 (2000) 657–668.
[84] T.V. Chalikian, A.P. Sarvazyan, G.E. Plum, K.J. Breslauer, Influence of base composition, base sequence, and duplex structure on DNA hydration: apparent molar volumes and apparent molar adiabatic compressibilities of synthetic and natural DNA duplexes at 25 degrees C (1994), Biochemistry 33 (1994) 2394–2401.
[85] T.V. Chalikian, J. Völker, A.R. Srinivasan, W.K. Olson, K.J. Breslauer, The hydration of nucleic acid duplexes as assessed by a combination of volumetric and structural techniques, Biopolymers 50 (1999) 459–471.